LNF-91/043 (R)
8 Luglio 1991

Juliet Lee-Franzini:

CUSB @ DAΦNE ?

Presented at the
Workshop on Physics and Detectors for DAΦNE
Frascati, April 9-12, 1991

INFN - Laboratori Nazionali di Frascati
Servizio Documentazione

LNF-91/043 (R)
8 Luglio 1991

CUSB @ DAΦNE ?

Juliet Lee-Franzini
SUNY at Stony Brook, Stony Brook, New York 11794

ABSTRACT

A very compact precision electromagnetic spectrometer, the CUSB-II detector, which has been used with great success to study Υ spectroscopy, search for exotic particles and measure properties of the B and B^* mesons at the Cornell Electron Storage Ring, is described. It seems to be an ideal instrument for tuning up DAΦNE as it is being commissioned and for the performance of the first spectroscopic experiments.

1. Introduction

The CUSB-II detector is a highly segmented non-magnetic electromagnetic calorimeter consisting of BGO and NaI crystals and lead glass blocks.[1] Charged particle tracking and shower centroid information are provided by a drift chamber, silicon pads, and proportional chambers with cathode strip readouts. The detector is surrounded by a system of scintillation counters for muon triggers and endcaps for lepton triggers to allow precision photon energy determinations in the central calorimeter. The figure is a perspective drawing of the whole detector. The muon counters are partially cut out and the endcap is moved away from the central detector. We also show a close view of the BGO cylinder. A quadrant of the cylinder is partially unstacked so that some silicon detector modules become visible.

2. Detector Components

The heart of the CUSB-II detector is the bismuth germanate ($Be_4Ge_3O_{12}$, BGO) calorimeter, 11.6 X_0 deep, nested within the existing CUSB-I NaI array.[2] The trapezoidally shaped crystals are arranged in a cylindrical geometry. Thirty-six crystals, each covering 10° in azimuth (ϕ) and 45° to 90° in colatitude (θ), form a cylindrical shell around the beam pipe. Five concentric shells form one detector half. The crystals are viewed end on by miniature photo multiplier tubes (PMT); their other ends butt against the identical second polar half of the detector. The inner radius of the BGO cylinder is 8.3 cm, the outer radius 22.3 cm. The crystals in the three inner layers are 2 X_0 thick, the ones in the two outer layers are 2.8 X_0 thick. The array covers 70% of the solid angle, 0–360° in ϕ and 45°–135° in θ. Projective geometry together with longitudinal and azimuthal segmentation allow recognition of energy deposition patterns which is of great importance in particle identification.

The NaI array consists of 320 rectangular thallium doped NaI crystals in a square geometry. It is divided into four quadrants, each covering 90° in ϕ and 45° to 135° in θ. Each of the four quadrants consists of five layers of crystals. Each layer is eight crystals wide and is divided into two polar halves. The inner four layers have a thickness of 2.8 cm (1.1 X_0), the outer layer of 10.2 cm (3.9 X_0), for a total thickness of 8.3 X_0 at normal incidence. The crystals are viewed through a quartz window by PMT's. Every NaI quadrant is backed up by an array of 8×8 lead glass total absorption Čerenkov counters read out by PMT's. The dimensions of the lead glass blocks are $15.0 \times 15.0 \times 17.5$ cm^3. Their thickness corresponds to 7.7 X_0.

In order to minimize noise we use preamplifiers in the PMT base for BGO crystals. The PMT's are operated with grounded cathode and anode at typically 600 V. The voltage divider chain carries about 100 μA, thus the PMT gain falls at high light levels seen e.g., during injection. Peak and average (over 1 μsec) anode full scale signal currents (corresponding to 2–4 GeV energy deposition) are 100 and 20 μA, respectively. The long term anode average current is 10–100 pA. The preamplifier can be isolated from the PMT anode by a low capacitance, series-parallel FET switch, to measure noise and pedestals. The equivalent amplifier input noise charge is about 0.5 fC or 3100 electrons, equivalent to 50 keV energy deposit. At the line driver output the full scale differential signal is approximately 1 V. There are over 1000 PMT's in the calorimeter and each one of them has its own computer controlled high voltage power supply. Each of these supplies consists of a DC to DC converter with a negative feedback control loop, and

two 8-bit DAC's with a register each, one for coarse and the other for fine adjustment of the high voltage. The digital settings stored in the registers are converted to a voltage of 1.9 V (1.5 V) full scale for coarse (fine) adjustment and fed into the DC to DC converter, which produces an output voltage of up to 1.2 kV. One least count of the digital settings corresponds to 0.1 V at the output of the DC to DC converter.

A small drift chamber is located inside the BGO cylinder to provide charged particle tracking. It is constructed directly on the aluminum beam pipe which has a radius of 5 cm and is 1.6 mm thick. The outer radius of the chamber is 7.5 cm and its length 24 cm, thus subtending 85% of the solid angle. All wires are strung parallel to the beam direction. The θ-coordinate of tracks is measured by 40 cathode pads on the inner and outer surfaces of the chamber. The 72 sense wires and 240 strips are read out for timing and pulse height. Beam pipe and drift chamber together are 0.06 X_0 thick at normal incidence. The position resolution in the ϕ-coordinate is typically 150 μm. The rms angular resolution of the chamber is 0.5° in ϕ and about 10° in θ. The resolution is limited by the finite size of the beam spot, which is 600 μm wide in the plane of the storage ring and 1.5 cm long in beam direction.

Silicon pads (reverse biased surface barrier silicon detectors) are placed between the first and second layer of BGO to measure the θ-coordinate of shower centroids. There are 72 such elements, one behind every crystal in the first layer of BGO. The charge sensitive preamps and the cable drivers are realized in surface mount technology to minimize their volume. The position resolution along the beam direction is 8 mm for the pads which are made of two diodes and 4 mm for all other pads.

Between the five layers of NaI there are four planes of multiwire proportional chambers with cathode strip readouts to provide position measurements of shower centroids and minimum ionizing particles. They cover the same solid angle as the NaI array. For muons the position resolution obtained from centroids of the strip signals is 1–3 mm for the ϕ and θ-coordinates which translates into an angular resolution of about 2°.

The muon counters are a system of scintillation counters surrounding the calorimeter segmented in azimuth and arranged in a square geometry around the lead glass blocks. Located behind 2.5 nuclear interaction lengths (λ_0) of material they detect penetrating particles. We use them to trigger on collinear muon pairs. To detect a muon pair the muons must together cross 5 λ_0. There are a total of 35 counters, 6 on the two sides, 32 × 132 cm^2 in size, 12 on top and 11 below the calorimeter, 16 × 140 cm^2 in size. They cover 30% of the solid angle. The resolution for the time difference between hits

in $e^+e^- \to \mu^+\mu^-$ events, corrected for the z-position of the muon counter hits, is 1.8 ns.

Plastic scintillator endcaps are used to increase the solid angle for two nearly collinear leptons from Υ decays. It consists of 104 trapezoidally shaped scintillator wedges, arranged in three concentric rings around the micro-beta insertion magnets on both ends of the detector. They cover a large part of the solid angle that is not covered by the calorimeter. The inner radius of the endcap is 16.2 cm, the outer radius 85.0 cm for a polar angle coverage of 10°–47° and 133°–170°. There are 6 X_0 of lead between the interaction region and the scintillators. We measure the hit time with a resolution of 0.7 ns.

3. Signal Processing Electronics

Some 4,500 analog signals are brought out differentially from the detector to a radiation safe area, where they are shaped, digitized and then transferred to a computer which saves all events of interest on tape. The calorimeter signals are filtered by integration and differentiation respectively. The integrator is discharged with a time constant of 20 μs to avoid saturation. The integrator output is double-sampled providing pile up protection. One sample is taken just before signals arrive at the integrator to measure the base line and the other sample when the shaped signal reaches its maximum. For BGO signals the time difference between the two samples is 1.2 μs, for NaI it is 800 ns and for lead glass 300 ns. The digitization time is 20 μs per channel. For the BGO channels the energy scale has been set to 40 keV per ADC count. This results in a full scale of 2.5 GeV which accommodates the largest signals while maintaining precision at low energies. For the first two planes of NaI the full scale is 700 MeV and for the remaining planes it is 1.5 GeV. Channel to channel variations have been measured with a precision pulser system to better than 0.5%.

TDC's used for drift chamber and muon counter timing have one TDC count equaling 1.5 ns and the full scale is approximately 3 μs. In the drift chamber, 1.5 ns correspond to a drift distance of 75 μm. A TDC channel can store up to eight hits for up to 3 μs. After every trigger a time signal is generated to read out the last stored hit.

In CESR there are seven bunches of electrons and of positrons, resulting in interactions every 365 ns in the center of the detector. At every beam crossing signal processing is started. If no trigger fires all integrators are reset to be ready for the next crossing. If a trigger occurs the signals are digitized, read out and processed by the on-line programs. The relative advance of the beam crossing signal allows for the necessary gates

to be generated before signals from the detector reach the electronics. The trigger logic is the logical or of four individual trigger criteria, the BGO total energy trigger, the two-muon trigger, the distributed energy trigger, and the endcap trigger. They all use the calorimeter signals provided by the pick off amplifiers in the calibration system. These signals are shaped to peak about 150 ns after beam crossing time, summed by analog adders and then discriminated. We use dual threshold discriminators; the timing is determined with a low threshold (V_{lo}) while a higher threshold (V_{hi}) determines the energy level. The output of the discriminator is sampled by the beam gate which is open for 70 ns around the time at which triggers from the latest beam crossing are expected.

The data acquisition system is fully automated. A run is started when the data micro-computer receives information from the CESR computers that stable running conditions have been achieved. Whenever a trigger occurs the digitized data is sent over the transport system to a dedicated micro-controller which writes the event into the 512 kbyte memory of the data micro-computer system using direct memory access. An event contains up to 16 kbytes so that the memory can hold up to 32 events. The data micro-computer then transfers the data to a buffer in a dedicated μVAX3200 which sends the event to one of a cluster of 14 μVAX3100s, to perform the on-line data processing. The data are filtered to reject events from beam-gas and beam-wall interactions. The analysis also categorizes the events into Bhabha scattering events, hadronic events and dimuon events. For data storage we use 8 mm tapes. It takes approximately 22 ms to read an event into the buffer on the Intel system. At a trigger rate of 1.5 Hz, this results in a dead time of 33 ms in a second or 3.3%.

4. The Calibration System

To maintain the excellent resolution of the calorimeter we need to continuously monitor the small drifts in the PMT gains while taking data. For this purpose CUSB has developed a unique calibration system. It uses low energy monochromatic photons from radioactive sources embedded between crystal layers. Calibration data is taken within a window of 170 ns between beam crossings. A separate high sensitivity data path, is used to acquire calibration data. Two to three calibration cycles are taken per run. In BGO we obtain 12.1%, in NaI 8.2% rms resolution for the 1.17 and 1.33 MeV photons from ^{60}Co sources.

5. On-Line Data Processing

The longitudinal segmentation of the calorimeter allows the identification of particles by their energy deposition patterns. Electrons, positrons, and photons generate electromagnetic showers through radiation and pair production, losing all their energy in 10–20 radiation lengths. The longitudinal profile of the energy deposition due to these showers shows a sharp initial rise due to the exponential increase of the number of particles. After a broad maximum the shower will decline gradually. The shower also spreads in transverse direction. To distinguish between showers caused by electrons or positrons and showers caused by photons we search for drift chamber tracks pointing to the shower, indicating that it has been caused by a charged particle.

For all other charged particles dE/dx is approximately constant. A minimum ionizing particle from an e^+e^- collision deposits an amount of energy, proportional to the thickness of the crystal, in all crystals of a single sector in the calorimeter. Such a pattern of energy deposition we call a "track". If the particle is a hadron it can also undergo nuclear reactions, which may cause the track to end with a single large energy deposit. We identify hadronic events by the presence of tracks in the calorimeter. Muons do not interact strongly with the nuclei and penetrate the whole calorimeter if their kinetic energy is large enough. Our muon identification is therefore based on the observation of a track which penetrates both the BGO and NaI arrays and causes a hit in the muon counters.

6. Detector Performance

We monitor the performance of the detector using Bhabha scattering events. The energy spectrum is peaked at 99% of the beam energy of 5.18 GeV with an energy resolution of 0.91%. The excellent agreement of the peak position with the beam energy shows that this calibration can indeed be extrapolated over many orders of magnitude to measure the energy of 5 GeV electrons.

We have checked the energy resolution for low energy photons using low multiplicity events: the process $\Upsilon(3S) \to \chi_b(2P_J) + \gamma$, obtained from an analysis of the cascade process $\Upsilon(3S) \to \chi_b(2P_J)\gamma \to \Upsilon(1S,2S)\gamma\gamma$, followed by $\Upsilon \to \mu^+\mu^-$ or $\Upsilon \to e^+e^-$.[3] The efficiency for the detection of these events (including trigger efficiency and acceptance) is about 10% for the e^+e^- channel and 15% for the $\mu^+\mu^-$ channel. The fitted resolution has an rms width for the gaussians of $\approx$2% of their mean.

The reaction $\Upsilon(3S) \to \Upsilon(2S,1S)\pi^0\pi^0$ can be isolated by selecting events with four

photons and a nearly collinear e^+e^- or $\mu^+\mu^-$ pair in the detector. The leptons are from the decay of the final state Υ. In the spectrum of the sum of all photon energies we observe peaks at 330 MeV and 880 MeV, due to the transitions to $\Upsilon(2S)$ and $\Upsilon(1S)$. The efficiency for detecting these events with all particles sufficiently isolated is about 4%. To confirm that the photons are indeed from the decay of π^0's we form all possible photon pairs and calculate their invariant masses. We determine the polar angle of the photons using the silicon detector which has an efficiency of 40–60% for photons below 1 GeV. We observe a peak in the invariant mass spectrum at 135 MeV, in agreement with the π^0 mass. The invariant mass resolution is $\approx$9% at 135 MeV.

7. Conclusion

We have described a precision electromagnetic spectrometer which has achieved an energy resolution of 1% at 5 GeV and 2% at 100 MeV, sufficient to resolve the fine structure of the $\chi_b(2P_J)$ states in the transitions $\Upsilon(3S) \rightarrow \chi_b(2P_J)\gamma$. We have successfully used this detector to study the spectroscopy of the Υ system and properties of B mesons. Our results include measurements of the branching ratios of electric dipole and hadronic transitions between $b\bar{b}$ bound states, the fine structure of the $\chi_b(2P_J)$ states,[3,4] and measurements of the branching ratios of $\Upsilon(^3S)$ states to $\mu^+\mu^-$ pairs.[5] We have also searched for exotic particles in radiative decays of Υ's[6] and direct photons from the Υ(4S).[7] The properties of B mesons which we have studied are their semileptonic branching ratios, hyperfine splitting and B_s production at the $\Upsilon(5S)$ resonance.[8] We have performed a preliminary study of using CUSB for ϕ spectroscopy[9] at DAΦNE, found it highly feasible, and are now performing a complete Monte-Carlo simulation for the process $\phi \rightarrow \gamma + f_0(985)$.[10]

ACKNOWLEDGEMENTS

The author wishes to acknowledge her CUSB collaborators: U. Heintz, D. M. J. Lovelock, M. Narain, R.D. Schamberger, J. Willins, and C. Yanagisawa Stony Brook and P. Franzini, P.M. Tuts of Columbia University, for the work presented here and thanks them for the joy of having worked together so closely and synergetically for the past years. I also wish to thank Paolo Franzini for discussions, Paula Franzini and Meenakshi Narain for help in writing this paper. Finally, I wish to thank the organizers of this workshop for a most enjoyable and productive meeting. This research is supported by the US National Science Foundation.

REFERENCES

1. J. Lee-Franzini, Nucl. Inst. Meth. **A263**, 35 (1988); P. M. Tuts, Nucl. Inst. Meth. **A265**, 243 (1988).
2. P. Franzini and J. Lee-Franzini, Physics Reports **81**, 239 (1982).
3. U. Heintz et al., Phys. Rev. Lett. **66**, 1563 (1991).
4. M. Narain et al., submitted to Phys. Rev. Lett (1991); D. M. J. Lovelock, Ph.D. thesis, SUNY at Stony Brook, unpublished.
5. T.M. Kaarsberg et al., Phys. Rev. Lett. **62**, 2077 (1989) and Phys. Rev. D**35**, 2265 (1987).
6. P.M. Tuts et al., Phys. Lett. B**186**, 233 (1987).
7. M. Narain et al., Phys. Rev. Lett. **65**, 2749 (1990).
8. C. Yanagisawa et al., Phys. Rev. Lett. **66** 2436 (1991); J. Lee-Franzini et al., Phys. Rev. Lett. **65**, 2947 (1990).
9. J. Lee-Franzini, DAΦNE workshop proceedings, February, 1991.
10. U. Heintz et al., work in progress.

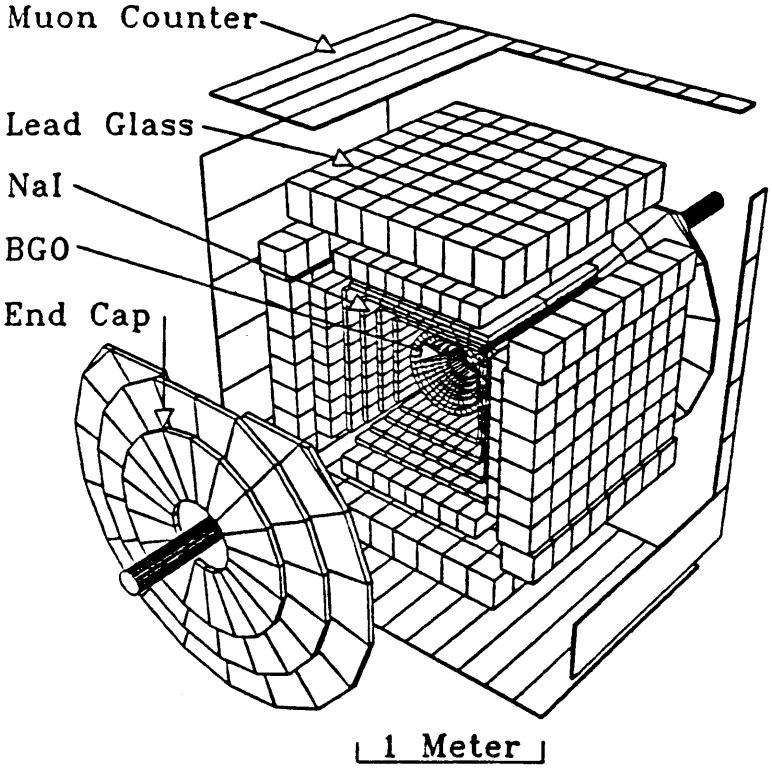
Muon Counter
Lead Glass
NaI
BGO
End Cap
1 Meter

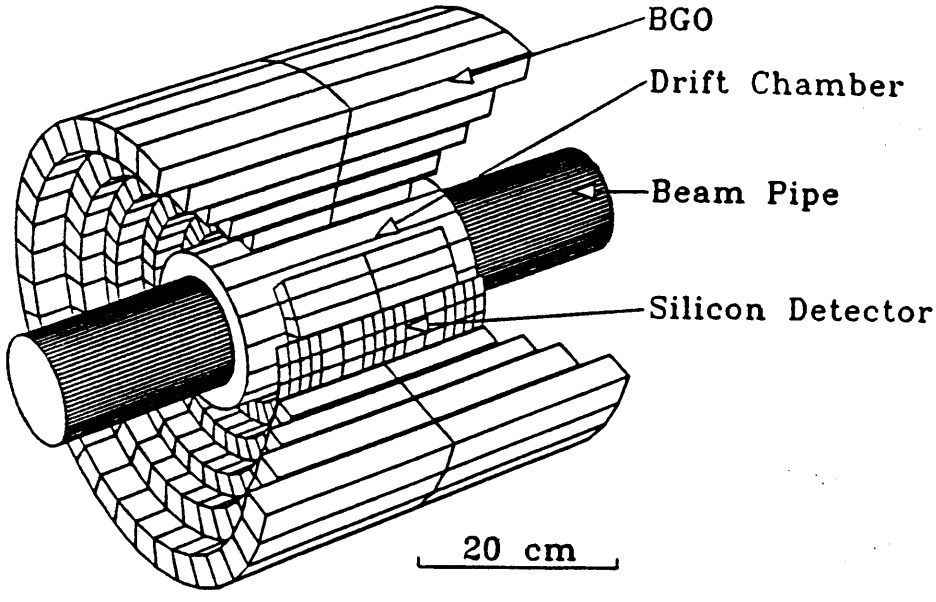
BGO
Drift Chamber
Beam Pipe
Silicon Detector
20 cm

CUSB-II